Morphology of polyoxymethylene-based polymer alloys

Shuichi Takamatsu, Tomomi Kobayashi and Tadashi Komoto*
Department of Materials Engineering, Gunma University, Tenjin-cho, Kiryu, Gunma 376, Japan

and Motoyuki Sugiura and Kazumine Ohara
Nippon Oil and Fats Co. Ltd, Taketoyo-cho, Chita, Aichi 470-23, Japan
(Received 1 November 1993; revised 16 February 1994)

A transmission electron microscopic study was carried out on polymer alloys of polyoxymethylene (POM) with low density polyethylene (LDPE) and styrene/acrylonitrile-grafted LDPE (LDPE-*g*-PSAN) from the point of view that the compatibility of POM and LDPE will be improved by the grafted PSAN chain which has a solubility parameter close to that of POM, though POM and LDPE are immiscible with each other. Low temperature plasma etching followed by the carbon replica method were applied to examine the size and distribution of particles in LDPE and LDPE-*g*-PSAN in POM matrices by TEM. The size distribution curve of the dispersed particles had its maximum at a particle diameter of $\sim 1.5\,\mu m$ for LDPE and $\sim 0.2\,\mu m$ for LDPE-*g*-PSAN. It was also found from the TEM morphologies that the interaction of the particles with the POM matrix is stronger for LDPE-*g*-PSAN than for LDPE. This is accounted for by a difference in their solubility parameters.

(Keywords: polymer alloy; polyoxymethylene; polyethylene)

INTRODUCTION

Many immiscible polymer alloys are used as industrial materials. Immiscible polymers with highly different chemical natures tend to be phase-separated to a large extent, which leads to deterioration of their properties in many cases. Addition of a third component, a miscibility improving agent, to an immiscible polymer blend is promising to improve the blend properties. The miscibility improving agents are in general random, block and graft copolymers obtained from monomers with different chemical natures[1-3]. Block and graft copolymers as miscibility improving agents may be unreactive types such as polystyrene–poly(methyl methacrylate) block copolymers for polystyrene/poly(methyl methacrylate) blends[4] and polypropylene–polyamide graft copolymers for polypropylene/polyamide blends[5] and reactive types such as ionomers or carboxylated polyethylenes for polyamide/polyethylene blends[6] and carboxylated polypropylenes for poly(ethylene terephthalate)/polypropylene blends[7].

Polyoxymethylene (POM) and low density polyethylene (LDPE) are an immiscible polymer pair, because they are very different in polarity as is evident from the large difference in their solubility parameters (11.1 and $\sim 8.0\,cal^{1/2}\,cm^{-3/2}$, respectively)[8]. These polymers are, however, of importance for industrial uses and accordingly their polymer alloys with improved miscibility and properties will be of interest for various applications.

Recently, unique block and graft copolymers have been developed for miscibility improving agents using particular peroxide compounds, where the trunk polymer is composed of polyolefins and the graft polymer is vinyl polymers[9,10]. This method was also applied to the synthesis of a graft copolymer with LDPE as the trunk polymer and styrene–acrylonitrile copolymer (PSAN) as the graft. The resultant graft copolymer, designated LDPE-*g*-PSAN, was used as a miscibility improving agent for POM and LDPE, because the graft chain PSAN may interact strongly with POM as the matrix of the polymer alloy.

It is, therefore, of interest to investigate the morphology of such a particular POM-based polymer alloy containing LDPE-*g*-PSAN in comparison with that of a POM/LDPE blend. Low temperature plasma etching may give important information on the morphology of the two polymer systems. Hansen *et al.*[11] measured rates of weight loss of various polymers by their reaction with oxygen plasma. It is reported that the rate of weight loss of POM is ~ 2.5 times that of LDPE. Therefore, phase-separated particles consisting of LDPE will remain on the specimen surface after etching. TEM of carbon replica films obtained from the etched surfaces will be reported in this paper.

EXPERIMENTAL

Specimens

Styrene (70 wt%) and acrylonitrile (30 wt%) were copolymerized in the presence of t-butyl peroxycarbonyloxyethyl methacrylate (3 wt% of the total vinyl monomers) as they were mixed with LDPE ($M_n = 16\,100$ and

* To whom correspondence should be addressed

0032-3861/94/17/3598-06

$M_w = 216000$) at ~80°C, resulting in the formation of a PSAN precursor ($M_n = 120000$ and $M_w = 360000$), a random copolymer having pendent t-butyl peroxide groups. The mixture of PSAN (30 wt%) and LDPE (70 wt%) thus obtained was melt-blended at 200°C, where the peroxide groups were decomposed and the resultant peroxy radicals eliminate hydrogen atoms from LDPE in the molten state. This gives rise to the formation of the graft copolymer LDPE-*g*-PSAN[10]. As the graft copolymer is formed by a polymer (LDPE)/polymer (PSAN) reaction, the reaction product may contain unreacted polymers. It was difficult to remove them from the reaction product for lack of a suitable solvent for their fractionation.

Two polymer alloys were prepared by blending POM (90 wt%) with LDPE (10 wt%) and LDPE-*g*-PSAN (10 wt%) in the molten state at 200°C in a twin-screw extruder. The POM used in this study was Duracon M90-10. The polymer alloys melted at 210°C were then injection moulded at 80°C. It is noted that the POM/LDPE and POM/LDPE-*g*-PSAN blends were turbid in the molten states, indicating phase-separated melt systems. The injection-moulded specimens were subjected to morphological experiments.

Low temperature oxygen plasma treatment

The polymer specimen was trimmed by a stainless steel knife and then cut by a glass knife, spraying cold nitrogen gas, in an ultramicrotome to obtain an inner morphology of the specimen. The specimen thus obtained was subjected to low temperature oxygen plasma etching under the following conditions: power, 20 W and 100 mA; frequency 13.56 MHz; etching time, 5 and 30 min; pressure, 0.1 Torr (~13 Pa).

Carbon replication

Carbon shadowing was carried out *in vacuo* on the plasma-treated surface of the specimen at an angle of 30° by an arc discharge of carbon electrodes. Oxygen plasma treatment was also carried out on the coated carbon to make it hydrophilic. A drop of concentrated aqueous gelatin solution was then placed on the specimen surface. After being completely dried, the gelatin was peeled off the specimen, where the very thin surface layer of polymer and coated carbon adhered to the gelatin. The gelatin was placed upside-down on an aqueous KSCN solution to dissolve, leaving a carbon replica film with the polymer surface layer on the surface of the solution. The replica film was then washed twice with distilled water and collected on a copper grid for TEM observation.

TEM observation

The carbon replica films thus obtained were subjected to TEM observation in a Hitachi H 300 transmission electron microscope with an accelerating voltage of 75 kV.

Estimation of the size and number of particles in alloys

As will be mentioned in the following section, LDPE and LDPE-*g*-PSAN were dispersed as particles in their alloys with POM. The size and number of the particles were estimated from TEM micrographs. A size distribution was measured for 196 LDPE particles found in an area of 4755 μm^2 and 751 LDPE-*g*-PSAN particles in an area of 440 μm^2 of the TEM micrographs, respectively.

RESULTS AND DISCUSSION

Morphology of plasma-etched POM

Figure 1 shows a TEM micrograph of a carbon replica film of a 5 min plasma-etched surface obtained from the inner part of the POM sheet, where a smooth surface with orientation of POM crystals is seen. Radially oriented lamellar striations which are parts of a spherulite were also found (not shown).

Morphology of the plasma-etched POM/LDPE blend

Figure 2a shows a TEM micrograph of a carbon replica film of a 5 min plasma-etched surface obtained from the inner part of the POM/LDPE blend. Three kinds of circular textures are seen on the POM matrix.

The dark circular particles (A) in *Figure 2a* are LDPE. It is thought that the dark particles were transferred to the carbon replica film from the POM matrix in the replication process shown in *Figure 2b*, where the coating and peeling off process of gelatin is not shown. A LDPE particle in the POM matrix is sectioned by a glass knife, etched by oxygen plasma to some extent and then carbon-coated as is shown in the top of the figure, a cross-sectional view along a line X–Y of *Figure 2a*. In the case where the thickness of the glass knife-sectioned LDPE particle is about half the particle diameter or less, the sectioned particle is easily transferred to the coated carbon film by replication because of the very weak adhesive force between the two polymers with highly different chemical nature as is evident from their solubility parameters. Thus, the resultant replica film shown in the middle of *Figure 2b* should contain the sectioned LDPE particle, which is too thick (about one to several μm as is seen from the micrograph) to transmit the electron beam, being dark. The cross-sectional view of the POM matrix to be obtained after replication can be illustrated as in the bottom of the figure, where the sectioned LDPE particle is absent.

The circular areas labelled B in *Figure 2a* consist of a bright half (top left part) and a darker half (bottom right part). It is found from a detailed examination of the micrograph that the bright part is a shadow of carbon and the other part is darker than the former due to carbon

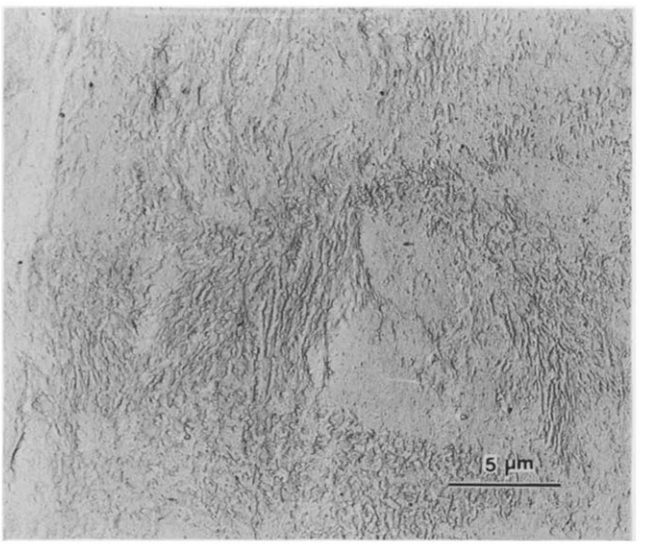

Figure 1 TEM micrograph of a carbon replica film of a 5 min oxygen plasma-etched surface of an inner part of the POM sheet

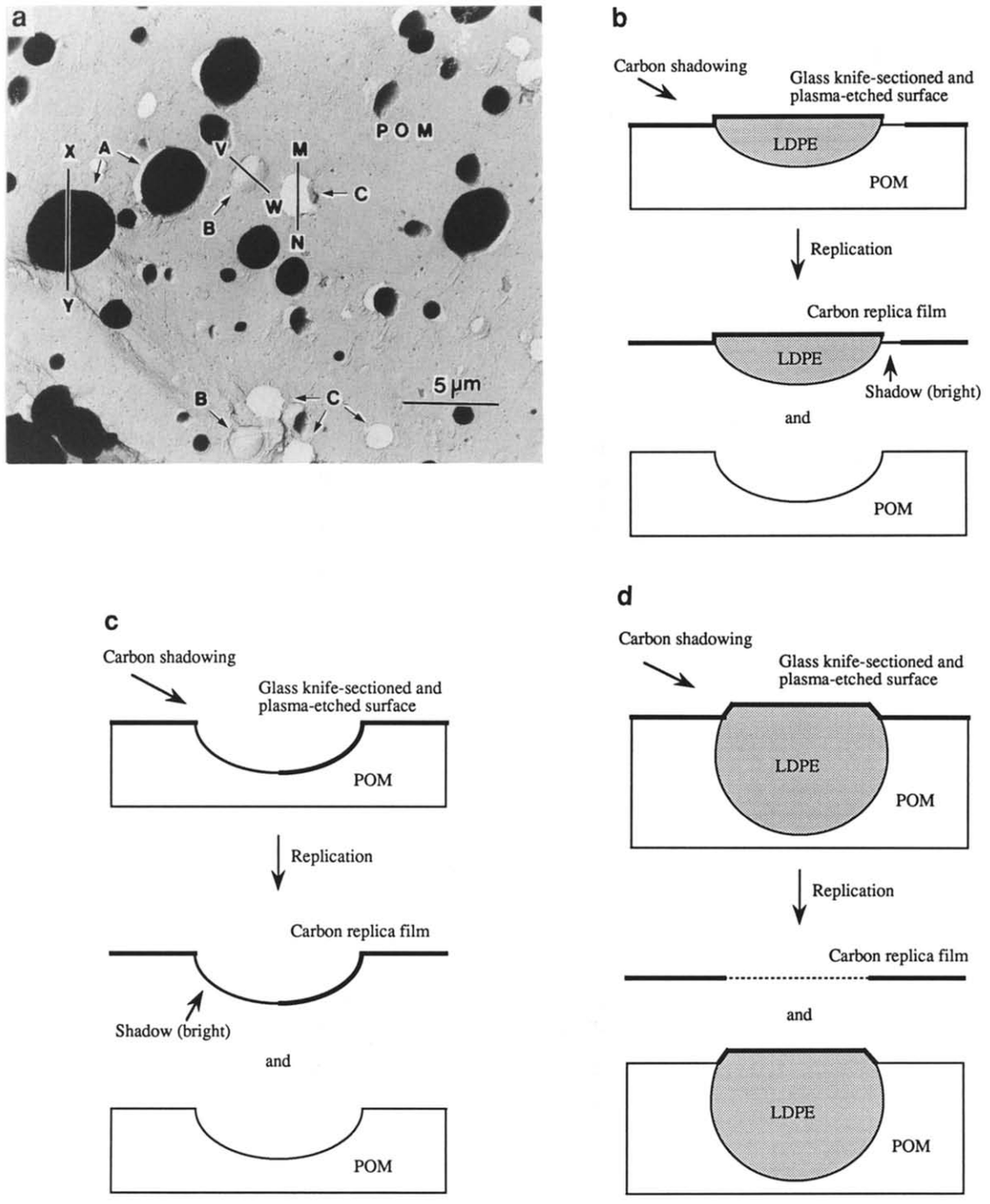

Figure 2 (a) TEM micrograph of a carbon replica film of a 5 min oxygen plasma-etched surface of an inner part of the POM/LDPE blend and schematic illustrations of cross-sectional views along lines (b) X–Y, (c) V–W and (d) M–N shown in (a) before and after replication

deposition. In other words, these circular textures are dimples or ghosts of spheres, say, ghosts of LDPE particles formed in such a way that a whole LDPE particle might be removed in the glass knife sectioning process from the POM matrix due to weak adhesion between the POM and the hemispherical LDPE surface with a small contact area. *Figure 2c* is a schematic diagram of a dimple and its carbon replica film as viewed along a line V–W of *Figure 2a*.

Homogeneously bright circles are labelled C in *Figure 2a*. In the case where the glass knife sectioning is done across the top part of a LDPE particle, a large part of the particle would remain embedded in the POM matrix as is shown in *Figure 2d*. Such an embedded, sectioned particle cannot be detached from the POM matrix in the replication process, because the particle is anchored by the surrounding POM matrix. It is also said that the only carbon deposited on the section of the LDPE particle was not transferred to the gelatin in the peeling process, giving rise to the formation of a hole in the replica film which is seen as the brightest area in the micrograph (*Figure 2d*). It is also found that part of a

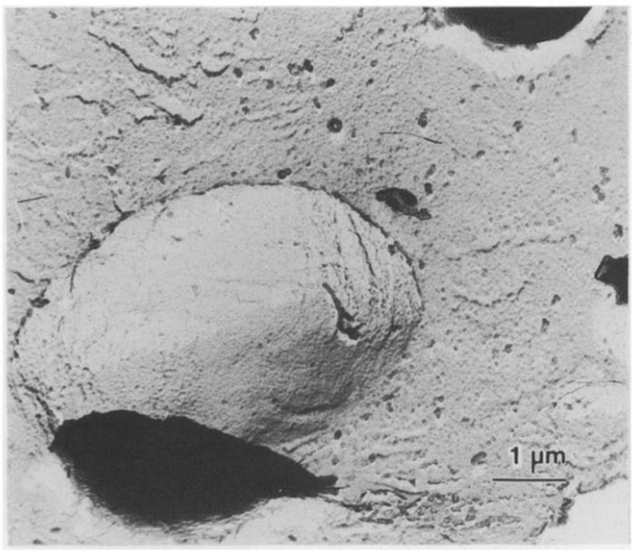

Figure 3 TEM micrograph of a dimple formed by glass knife sectioning for the POM/LDPE blend. Part of the LDPE particle remained in the dimple

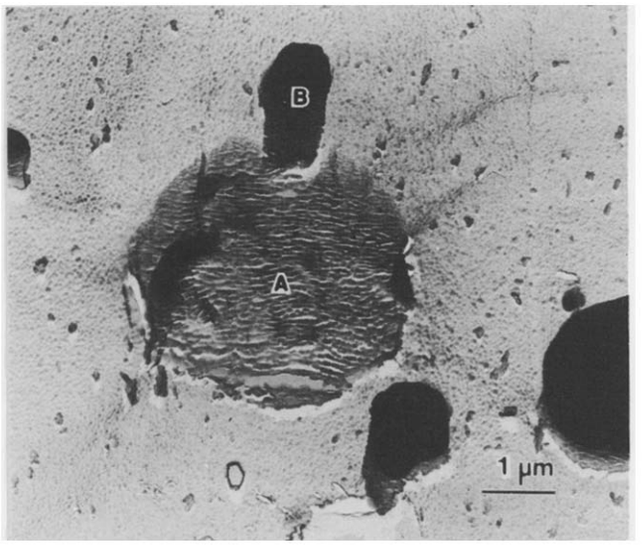

Figure 4 TEM micrograph of the LDPE surface layer with oriented morphology formed by sectioning and plasma etching

LDPE particle remained in a dimple after being sectioned and transferred to the carbon film by replication as shown in *Figure 3*.

As shown in *Figure 4*, some sectioned LDPE surfaces (A) were carbon replicated with neither transfer of LDPE particles from the POM matrix nor formation of holes, where the glass knife sectioning was done from top to bottom of the micrograph. This may be because that LDPE is so ductile (though cooled by cold nitrogen gas) that particles (B) are deformed by a shear due to sectioning, accompanying molecular chain orientations. Although particle A of *Figure 4* was not deformed so much, it is evident that LDPE chains on the sectioned surface were oriented because of the formation of striations 50–100 nm wide aligned perpendicular to the direction of sectioning. The striations are typical of a plasma etched surface morphology with oriented polyethylene because they are formed by a mechanism where the oriented polyethylene chains are broken by a reaction with oxygen plasma and accordingly the strained chains are relaxed accompanying rearrangement of the broken chains and recrystallization in the form of striations to which the molecular chains are perpendicular[12].

The morphology of the POM/LDPE blend surface sectioned by a glass knife and etched by further exposure to oxygen plasma was also investigated. *Figure 5* is a TEM micrograph of a carbon replica film of the blend etched by oxygen plasma for 30 min. *Figure 5* shows round and irregular shaped dark particles on the POM matrix with lamellar morphology. The dark round particles can be assigned to LDPE due to their similarity to those shown in *Figure 2a*. It is noted, however, that dark LDPE particles decreased in size and increased in number after 30 min plasma etching as is evident from *Figures 2a* and *5*. This can be accounted for by a weight loss, i.e. a thinning of each particle by the etching, and by an increase in depth of the POM layer etched at a rate of weight loss higher than that of LDPE. LDPE particles embedded deep in the POM matrix would appear on the etched POM surface in the course of etching, giving rise to an increase in number of LDPE particles after 30 min etching.

Morphology of the plasma etched POM/LDPE-g-PSAN alloy

Figure 6 shows a TEM micrograph of a carbon replica film of a 5 min plasma-etched surface obtained from the inner part of the POM/LDPE-*g*-PSAN alloy. It is noted that there were very few dark particles and lots of small, bright particles as compared with the (*Figure 2a*) POM/LDPE blend. The particles are obviously the LDPE-*g*-PSAN phase dispersed in the POM matrix. The thickness of the carbon-replicated layer of the glass knife-sectioned particle is thought to be so small that the darkness of the replica from the particle is comparable to that of the POM matrix. In other words, most of the sectioned particle might remain embedded in the matrix. This is evidence for strong adhesion between the LDPE-*g*-PSAN and POM.

The morphology of the glass knife-sectioned and plasma-etched surface of the copolymer particles was

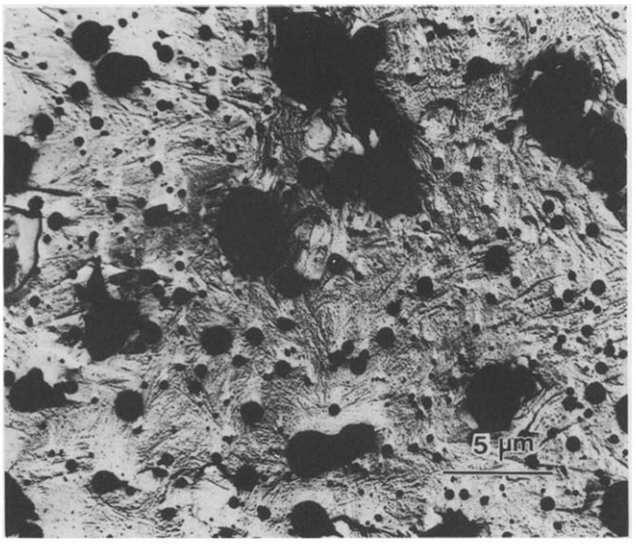

Figure 5 TEM micrograph of a carbon replica film of a 30 min oxygen plasma-etched surface of an inner part of the POM/LDPE blend

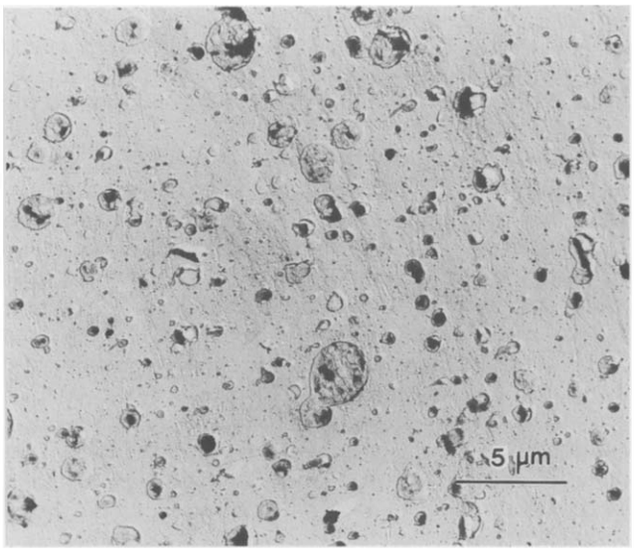

Figure 6 TEM micrograph of a carbon replica film of a 5 min oxygen plasma-etched surface of an inner part of the POM/LDPE-*g*-PSAN alloy

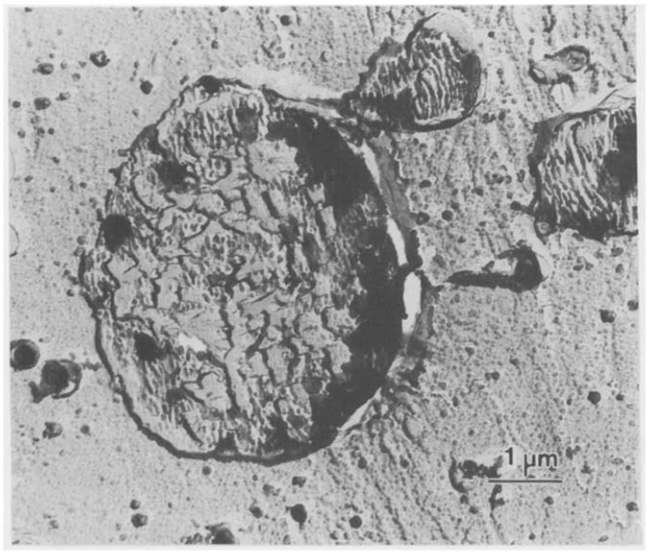

Figure 7 TEM micrograph of a carbon replica film of a 5 min oxygen plasma-etched surface of a sectioned POM/LDPE-*g*-PSAN particle

examined at a higher magnification (*Figure 7*). Two kinds of domains are seen in the micrograph. One is lamellar domains similar to the LDPE particles (although they were formed as an artifact in the TEM specimen preparation) and the other is flat domains. These lamellar and flat domains may be LDPE-rich and PSAN-rich phases, respectively. This is evidence for the possibility that the LDPE-*g*-PSAN phase is a mixture of the copolymer, LDPE and PSAN.

Figure 8 is a TEM micrograph of a carbon replica film of a 30 min plasma-etched surface obtained from the inner part of the POM/LDPE-*g*-PSAN alloy. Dark particles and bright particles with dark periphery are shown. It should be noted that the diameter of the dark particles is $< \sim 2\,\mu m$. The formation of dark particles $< \sim 2\,\mu m$ in diameter by the 30 min plasma-etching means that the POM matrix of this thickness or more, which had surrounded the LDPE-*g*-PSAN particles, was fully decomposed and the isolated particles, accompanying a decrease in their diameters, transferred to the carbon film by replication. On the other hand, it can be said that the bright particles with diameters of $> 2\,\mu m$ were formed by a mechanism where a thin surface layer transferred to the carbon film, while the greater fraction remained embedded in the POM matrix. This also supports an improved interfacial adhesive force between POM and the LDPE-*g*-PSAN copolymer, i.e. an improved compatibility of POM and LDPE.

Comparison of the size and number of dispersed particles

The size and number of 196 LDPE particles in an area of $4755\,\mu m^2$ in *Figure 2* were measured for the POM/LDPE alloy. The size distribution curve (solid line in *Figure 9*) of the LDPE particles indicates a maximum diameter of $\sim 7\,\mu m$ and has its maximum at a diameter

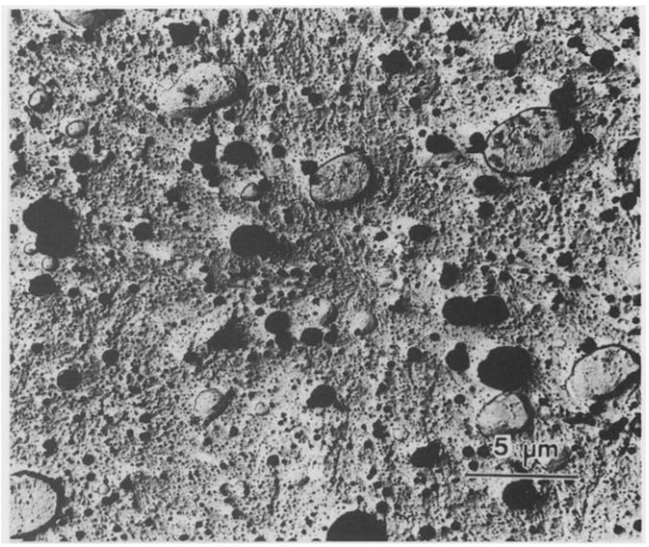

Figure 8 TEM micrograph of a carbon replica film of a 30 min oxygen plasma-etched surface of an inner part of the POM/LDPE-*g*-PSAN alloy

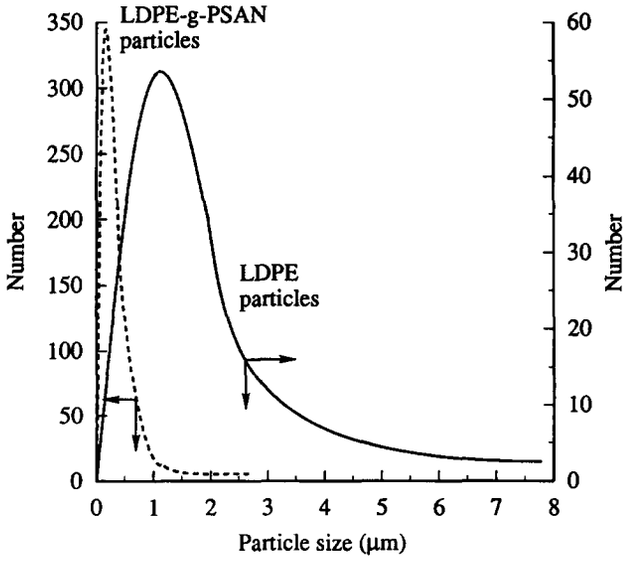

Figure 9 Distribution of the diameter of the dispersed particles in the POM/LDPE and POM/LDPE-*g*-PSAN systems: 196 LDPE particles in $4755\,\mu m^2$ and 751 LDPE-*g*-PSAN particles in $440\,\mu m^2$ were subjected to the diameter measurements

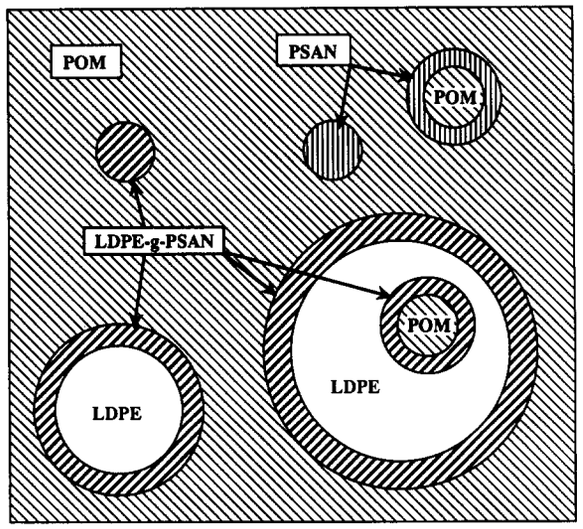

Figure 10 Schematic illustration of LDPE-*g*-PSAN particles dispersed in the POM matrix

of $\sim 1.5\,\mu m$. From the size distribution data, the total area of the sectioned surfaces of the LDPE particles is calculated as $711\,\mu m^2$ which is 14.9% of the area of $4755\,\mu m^2$. The area of the POM matrix is 85.1% of $4755\,\mu m^2$. These values should be same as the volume per cent of LDPE (14.9 vol%) and POM (85.1 vol%), respectively. Taking into consideration the density of $0.925\,g\,cm^{-3}$ for LDPE and $1.42\,g\,cm^{-3}$ for POM, the content of LDPE is calculated as 10.2 wt%. This value is very close to that (10 wt%) of the LDPE charged in the POM/LDPE alloy.

The size and number of 751 LDPE-*g*-PSAN particles in an area of $440\,\mu m^2$ of *Figure 6* were also measured for the POM/LDPE-*g*-PSAN alloy. The size distribution curve (broken line in *Figure 9*) has its maximum at a diameter of $\sim 0.2\,\mu m$ and the maximum particle diameter is $\sim 3\,\mu m$. The number of LDPE-*g*-PSAN particles with diameters $< \sim 0.1\,\mu m$ is underestimated, although the volume fraction is very small. The size distribution curves (*Figure 9*) clearly indicate that the dispersed particles are smaller in size and larger in number for the POM/LDPE-*g*-PSAN system than for the POM/LDPE system. From the size distribution data, the total area of the sectioned surfaces of the LDPE-*g*-PSAN is calculated as $115\,\mu m^2$, which is $\sim 26.1\%$ of the area of $440\,\mu m^2$. This means that the LDPE-*g*-PSAN content estimated by TEM is 26.1 vol%, which corresponds to 19.8 wt% assuming the density of LDPE-*g*-PSAN as $\sim 1.0\,g\,cm^{-3}$. This is almost twice the content (10 wt%) of the LDPE-*g*-PSAN charged in the alloy.

Structure of the dispersed POM/LDPE-g-PSAN alloy

According to the well known Flory–Huggins theory, different polymers are usually immiscible because of their very low combinatorial entropy for mixing. Polymer miscibility is, therefore, dependent on the other parameter, an interaction energy term, which is a function of the solubility parameter difference of the polymers. Polymers with close solubility parameters tend to be miscible with each other and a polymer with a solubility parameter intermediate to those of the component polymers tends to be a miscibility improving agent, localizing at the phase boundary.

It is, therefore, important to relate the state of dispersion of the particles with solubility parameters of the polymers used in this study. As was mentioned in the Introduction, POM and LDPE have solubility parameters of 11.1 and $\sim 8.0\,cal^{1/2}\,cm^{-3/2}$, respectively, the latter value being that for polyethylene. The immiscibility of POM and LDPE is clearly accounted for by their solubility difference. A good agreement of the LDPE content estimated from the TEM micrograph with that charged in the POM/LDPE alloy is also evidence for the immiscibility of LDPE and POM.

It is reported that the solubility parameters of polystyrene and polyacrylonitrile are ~ 9.1 and $12.5\,cal^{1/2}\,cm^{-3/2}$, respectively[8]. Thus, the solubility parameter of PSAN is calculated as $\sim 10.7\,cal^{1/2}\,cm^{-3/2}$ from the copolymer composition of styrene (70 wt%, i.e. 54 mol%) and acrylonitrile (30 wt%, i.e. 46 mol%). The value of $10.7\,cal^{1/2}\,cm^{-3/2}$ is very close to that for POM. This may suggest a miscibility of PSAN with POM to some extent and accordingly the separation of LDPE chains of the copolymer would be prevented to a large extent by the grafted PSAN chains.

It should be noted that many LDPE-*g*-PSAN particles may contain the unreacted LDPE and PSAN domains. The similar solubility parameters of POM and PSAN and the high LDPE-*g*-PSAN content (19.8 wt%) estimated by TEM may mean a possibility of inclusion of not only LDPE and PSAN but also POM molecules in the dispersed particles. It may be said that some large dispersed particles with LDPE-*g*-PSAN shells contain the unreacted LDPE cores in which are also contained small particles consisting of LDPE-*g*-PSAN shells and POM cores. The small dispersed particles are three kinds of particles (LDPE-*g*-PSAN; PSAN (shell) and POM (core); unreacted PSAN), although they were not characterized by TEM. As a result, the structure of the POM/LDPE-*g*-PSAN alloy can be schematically illustrated as shown in *Figure 10*. This gives rise to the formation of a large number of small particles of the copolymer dispersed in the POM matrix. It is therefore concluded that the LDPE-*g*-PSAN graft copolymer is a miscibility improving agent for LDPE and POM.

REFERENCES

1 Paul, D. R. and Barlow, J. W. *Polymer* 1984, **25**, 487
2 Akiyama, S. *Kobunshi* 1987, **36**, 216
3 Akiyama, S. *Kobunshi Kako* 1989, **38**, 5
4 Von Riess, G., Kohler, J., Tournut, C. and Banderet, A. *Makromol. Chem.* 1967, **101**, 58
5 Ide, F. and Hasegawa, A. *J. Appl. Polym. Sci.* 1974, **18**, 963
6 MacKnight, W. J., Lenz, R. W., Musto, P. V. and Somani, R. J. *Polym. Eng. Sci.* 1985, **25**, 1124
7 Subramanian, P. M. and Mehra, V. *Polym. Eng. Sci.* 1987, **27**, 663
8 Grulke, E. A. in 'Polymer Handbook' (Eds J. Brandrup and E. H. Immergut), 3rd Edn, Interscience, New York, 1989, Ch. 6
9 Yamamoto, T. *Kobunshi* 1986, **35**, 1010
10 Suzuki, N., Sugiura, M., Goto, H. and Yamamoto, T. *Kobunshi Ronbunshu* 1990, **47**, 63
11 Hansen, R. H., Pascale, J. V., De Benedictis, T. and Rentzepis, P. M. *J. Polym. Sci. A* 1965, **3**, 2205
12 Kojima, M. and Satake, H. *J. Polym. Sci., Polym. Phys. Edn* 1982, **20**, 2153